Biochemical and Biophysical Research Communications 421 (2012) 671–677

Contents lists available at SciVerse ScienceDirect

Biochemical and Biophysical Research Communications

journal homepage: www.elsevier.com/locate/ybbrc

# 8-Oxo-7,8-dihydrodeoxyadenosine: The first example of a native DNA lesion that stabilizes human telomeric G-quadruplex DNA

Manali Aggrawal, Hyun Joo, Wanbo Liu, Jerry Tsai, Liang Xue *

*Department of Chemistry, University of the Pacific, 3601 Pacific Avenue, Stockton, CA 95211, USA*

ARTICLE INFO

*Article history:*
Received 5 April 2012
Available online 19 April 2012

*Keywords:*
DNA lesions
G-quadruplex DNA
Thermal denaturation
DNA conformations

ABSTRACT

Native DNA lesions in general destabilize DNA secondary structures such as duplex and G-quadruplex because they disrupt optimized interactions in DNA defined by nature. In this paper, we report the first example of a native DNA lesion (8-oxo-7,8-dihydrodeoxyadenosine, OxodA) that stabilizes human telomeric G-quadruplex DNA. CD thermal denaturation studies explicitly displayed increased melting temperatures of telomeric G-quadruplex DNAs that contain OxodA(s) in different DNA loops, suggesting enhanced thermal stability. Conformation studies of G-quadruplex DNAs containing OxodA(s) in the loops using CD and native PAGE revealed that they adopt a similar antiparallel conformation in $Na^+$ but have much more versatile conformations in $K^+$. According to computational calculations, the observed stabilization may result from the tight binding of $K^+$ into the pocket formed by the O8 of OxodA and its loop. The study reported here may provide better understanding of the effect of DNA lesions on G-quadruplex stability and conformation.



## 1. Introduction

G-quadruplex DNA structures are constructed by stacking planar Hoogsteen hydrogen-bonded G-quartets on top of each other [1]. Potential unimolecular quadruplex-forming sequences in *Escherichia coli*, other prokaryotic genomes, and the human genome have recently been identified via systematic surveys [2,3]. Amongst all the G-quadruplex-forming regions, telomeric DNA that consists of 5′-d(TTAGGG) repeating units at the ends of chromosomes has attracted most attention. Intramolecular G-quadruplexes formed in the telomeric regions were proven to inhibit the binding of telomerase, a reverse transcriptase that is expressed in 80–85% tumor cells and is essential for the unrestricted growth of cancer cells [4]; therefore, they have become potential therapeutic targets for cancer intervention [5,6]. The conformation of telomeric G-quadruplexes under physiological conditions has been extensively studied because structure–function relationships may exist [7].

In our group, we are interested in investigating the effect of naturally occurring modified nucleotides (DNA lesions) on the structure of telomeric G-quadruplex DNA. The 3′ overhang of single-stranded telomeric DNA in principle is prone to oxidation because it is more accessible to damaging agents such as reactive oxygen species (ROS) than duplex DNA. The resulting DNA lesions may regulate the conformation and stability of G-quadruplex DNA. However, to our knowledge, such studies are scarce in literature. 8-Oxo-7,8-dihydrodeoxyguanosine (OxodG) is the only native DNA lesion in G-quadruplex DNA that has been studied [8]. Another close example is an analog (dSpacer) mimicking abasic sites present in G-quadruplex DNA [9,10]. Both OxodG and dSpacer destabilize the corresponding G-quadruplex DNA regardless of their locations in the loops or G-quartets. In the present work, we report an unexpected stabilization of telomeric G-quadruplex DNA (**1**, Fig. 1) when we systematically replaced deoxyadenosine (dA) in the loops with its oxidized form (8-oxo-7,8-dihydrodeoxyadenosine, OxodA). This is the first example of a native DNA lesion that augments the stability of G-quadruplex DNA. The observation reported here is quite significant and may reinstate a common belief on the role DNA lesions in the stabilization of G-quadruplex DNA.

## 2. Materials and methods

All the chemicals and phosphoramidites for DNA synthesis were purchased from Glen Research. The DNA oligonucleotides were synthesized on an Applied Biosystems 392 DNA/RNA synthesizer, purified by polyacrylamide gel electrophoresis (PAGE), and characterized using a Shimadzu AXIMA-CFT MALDI-TOF mass spectrometer. UV spectra were collected on a Varian Cary 100 Bio UV–vis spectrophotometer. Circular dichroism spectra were recorded on a JASCO J-810 spectropolarimeter. T4 polynucleotide kinase was obtained from New England Biolabs. [$\gamma$-$^{32}$P]-ATP was purchased from MP Biochemicals. Quantification of 5′-[$^{32}$P]-labeled

* Corresponding author. Fax: +1 209 946 2607.
*E-mail address:* lxue@pacific.edu (L. Xue).

0006-291X/$ - see front matter © 2012 Elsevier Inc. All rights reserved.
http://dx.doi.org/10.1016/j.bbrc.2012.04.059

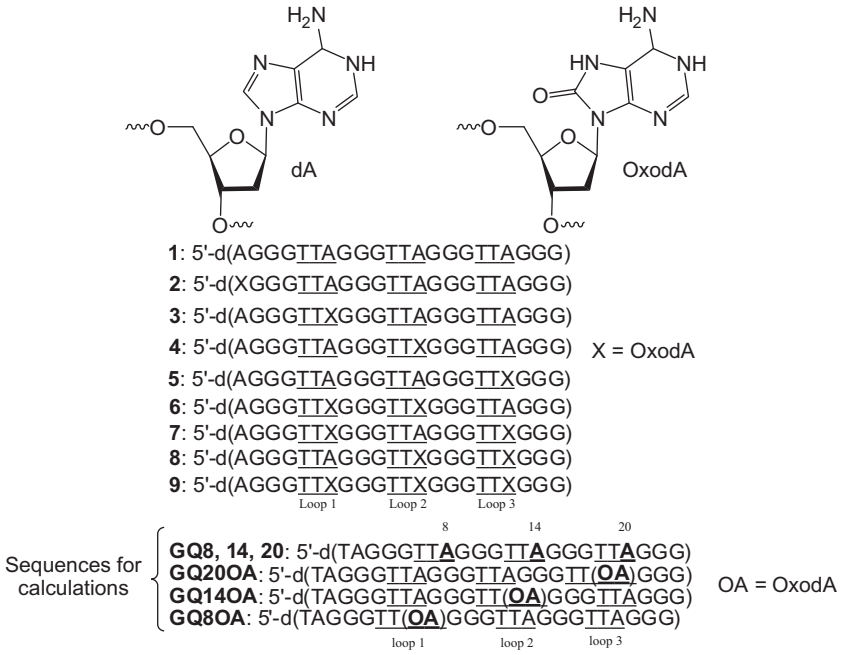


**Fig. 1.** G-quadruplex sequences used in this study.

oligonucleotides was carried out using a Storm 860 phosphorImager and ImageQuant 5.1 software (Molecular Dynamics).

CD and UV absorption spectra were determined in lithium cacodylate or phosphate buffer (10 mM, pH 7.0) with 10–150 mM KCl or NaCl. Native PAGE experiments were run at a 15% gel concentration and the gel results were measured by autoradiography.

The single point energy calculations on the optimized geometries were carried out at ONIOM(B3LYP/6-311++G(2d,p):UFF). The potassium ion binding energies of the G-quadruplexes at each adenine present in loop 1, 2, and 3 are calculated using a two-level ONIOM approach [11] that combines quantum mechanical (QM) methods and molecular mechanics (MM) methods (ONIOM(QM:MM)) implemented in the Gaussian 03 program package. The loop regions including each adenine base at position 8, 14, and 20 in the sequence are optimized at the QM level using the high-level density functional B3LYP/6-31G(d), and the rest portions of the sequences are treated using the low-level universal force field (UFF) MM methods (ONIOM(B3LYP/6-31G(d):UFF)). For the geometry optimization, the MM level geometries are frozen to avoid introducing errors from the force field; therefore, at each set only the QM level geometries are optimized and the MM energies only differ depending upon the geometry of the QM level.

## 3. Results

### 3.1. Thermal denaturation of G-quadruplex DNA containing OxodA

DNA sequences (**1**–**9**) containing zero, one, two, or three OxodAs (Fig. 1) were prepared using standard phosphoramidite chemistry. The thermal stability of G-quadruplex DNA (**1**–**9**) was determined using UV thermal denaturation in the presence of $Na^+$ or $K^+$ at different concentrations. The wavelength 295 nm was monitored as a function of increasing temperature [12]. The

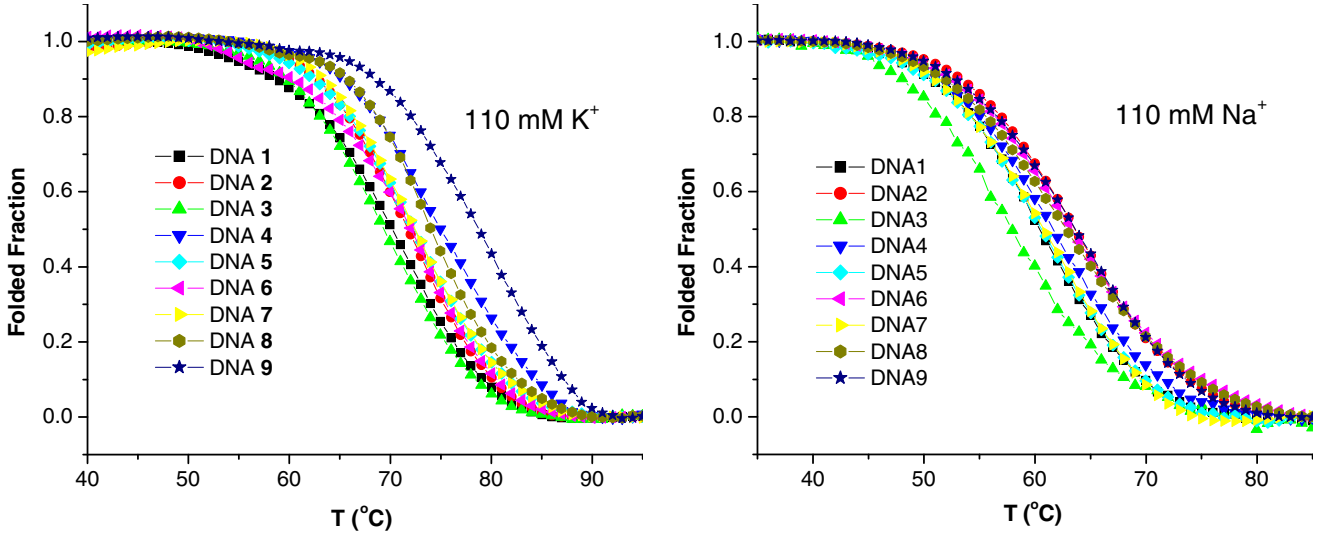


**Fig. 2.** Representative UV melting profiles of DNA **1**, **2**, **3**, **8**, and **9** in the presence of 110 mM $K^+$ (left) and $Na^+$ (right).

**Table 1**
Effect of OxodA on the thermodynamic properties of G-quadruplex DNA in 110 mM $Na^+$ and $K^+$.

| DNA | In buffered 110 mM NaCl solution | | | | In buffered 110 mM KCl solution | | | |
|---|---|---|---|---|---|---|---|---|
| | $\Delta H°$ (kcal/mol) | $\Delta S°$ (cal/mol) | $\Delta G°_{37}$ (kcal/mol) | $T_m$ (°C) | $\Delta H°$ (kcal/mol) | $\Delta S°$ (cal/mol) | $\Delta G°_{37}$ (kcal/mol) | $T_m$ (°C) |
| 1 | −51.84 ± 0.49 | −156 ± 1.47 | −3.60 ± 0.05 | 60.1 ± 0.04 | −48.63 ± 1.11 | −142 ± 3.25 | −4.57 ± 0.14 | 70.1 ± 0.16 |
| 2 | −49.36 ± 0.75 | −147 ± 2.22 | −3.87 ± 0.08 | 63.1 ± 0.04 | −57.32 ± 0.37 | −166 ± 1.07 | −5.78 ± 0.05 | 72.7 ± 0.62 |
| 3 | −48.35 ± 0.62 | −146 ± 1.86 | −3.07 ± 0.06 | 58.3 ± 0.35 | −54.38 ± 0.51 | −159 ± 1.51 | −5.12 ± 0.06 | 70.3 ± 0.27 |
| 4 | −47.92 ± 0.64 | −143 ± 1.92 | −3.41 ± 0.07 | 61.1 ± 0.04 | −53.35 ± 0.50 | −153 ± 1.44 | −5.84 ± 0.07 | 74.4 ± 0.27 |
| 5 | −53.19 ± 0.73 | −160 ± 2.20 | −3.66 ± 0.08 | 60.1 ± 0.00 | −53.04 ± 0.80 | −154 ± 2.31 | −5.34 ± 0.11 | 72.8 ± 0.40 |
| 6 | −45.29 ± 0.38 | −134 ± 1.14 | −3.61 ± 0.04 | 60.6 ± 0.40 | −50.13 ± 1.26 | −146 ± 3.66 | −4.98 ± 0.17 | 72.3 ± 0.13 |
| 7 | −44.34 ± 0.28 | −133 ± 0.84 | −3.13 ± 0.03 | 59.7 ± 0.64 | −56.95 ± 0.48 | −165 ± 1.39 | −5.85 ± 0.06 | 72.0 ± 1.36 |
| 8 | −46.60 ± 0.42 | −139 ± 1.27 | −3.60 ± 0.05 | 63.1 ± 0.20 | −52.24 ± 0.74 | −151 ± 2.14 | −5.49 ± 0.10 | 74.1 ± 0.12 |
| 9 | −49.84 ± 1.00 | −148 ± 2.97 | −3.90 ± 0.12 | 64.2 ± 0.04 | −53.43 ± 1.05 | −152 ± 2.99 | −6.25 ± 0.16 | 79.0 ± 0.05 |

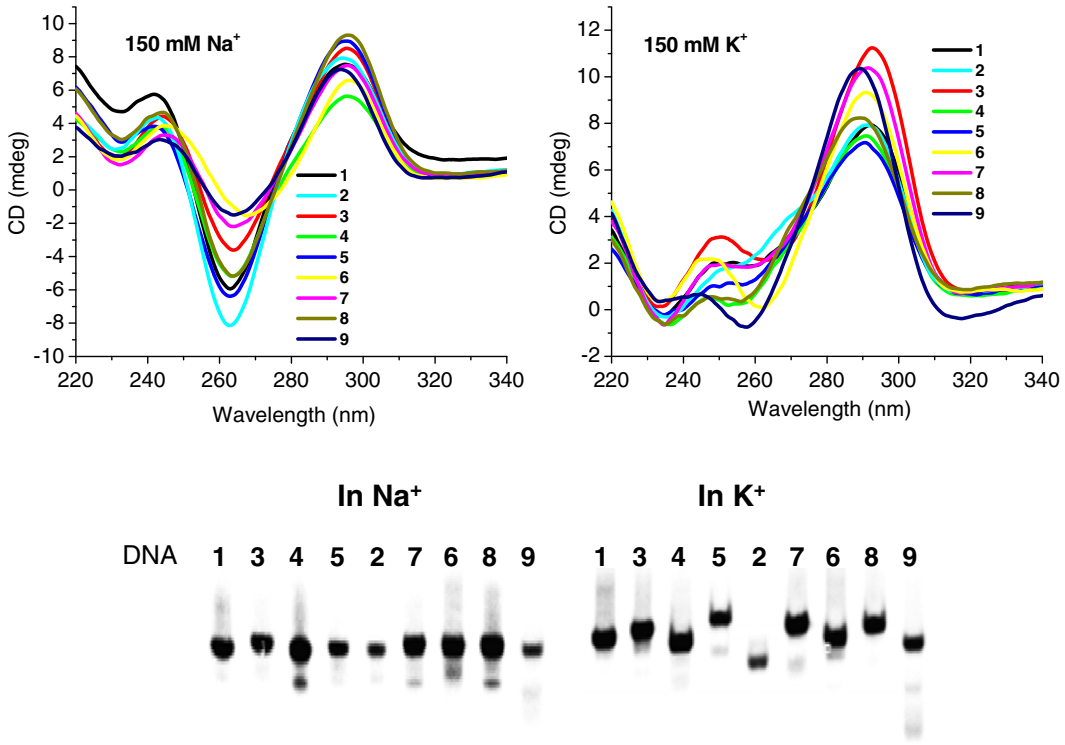


**Fig. 3.** Top: CD spectra of G-quadruplex DNA 1–9 in the presence of 150 mM $Na^+$ (left) and $K^+$ (right). Bottom: Mobility of G-quadruplex DNA **1**–**9** in $K^+$ (left) and $Na^+$ (right) determined by native PAGE.

melting temperature ($T_m$) of each DNA was determined by calculating the first derivative of its melting profile, representing the temperature at which 50% G-quadruplex DNA dissociates into random coils. The $T_m$ values were independent of DNA concentration between 1 and 5 μM [13]. At the rate of heating (0.2 °C/min) no apparent hysteresis between the melting and annealing profiles was observed [13]. Representative melting profiles of G-quadruplex DNA **1**–**9** in 110 mM $Na^+$ or $K^+$ are shown in Fig. 2. All G-quadruplex DNAs were more stable in $K^+$ than in $Na^+$, which is consistent with previous reports. In general, replacement of dA in the loops with OxodA increased melting temperatures of the corresponding G-quadruplex DNAs, suggesting their enhanced thermal stability. Increase in melting temperatures was somewhat dependent of the number and location of OxodA in the sequences. In 110 mM $K^+$, the melting temperatures of DNA **2**, **4**, and **5** that contain one OxodA at 5′ position, loop 2, and loop 3, respectively (Fig. 1), increased by 2.2–2.8 °C as compared to that of DNA **1**. In contrast, the melting temperature of DNA **3** containing OxodA in loop 1 only had a 0.2 °C increment. DNA **6**, **7**, and **8** containing two OxodAs had an increment of 1.9, 2.3, and 4.0 °C in melting temperatures, respectively. It is noteworthy that DNA **8** without OxodA in loop 1 had the highest stability amongst the three. The most significant stabilization was observed for G-quadruplex DNA **9** that contains three OxodA substitutions in the loop 1, 2, and 3, respectively, showing an impressive 8.9 °C increment of its melting temperature. The stabilization of G-quadruplex DNA by OxodA in $Na^+$ was weaker than in $K^+$. In 110 mM $Na^+$, increase in melting temperatures of G-quadruplex DNA **3**–**7** containing either one or two OxodAs was negligible. DNA **3** even showed a slight destabilization with a decrease in its melting temperature by 1.8 °C as compared to the control DNA **1**. In $Na^+$, only DNA **2**, **8**, and **9** displayed noticeable thermal stabilization effect by OxodA. More specifically, DNA **2** containing OxodA at 5′ position and DNA **8** containing OxodAs in loop 2 and 3 both had a 3.0 °C increment in their melting temperatures. DNA **9** containing three OxodAs in the loops increased its melting temperature by 4.1 °C as compared with DNA **1**. The thermodynamic values were derived from van't Hoff analysis of the melting profiles [12] and these are

summarized in Table 1. The values are comparable with those previously reported for intramolecular quadruplex DNA, which are typically between 15 and 24 kcal/mol per quartet [14].

### 3.2. Conformational studies of G-quadruplex containing OxodA by CD and PAGE

The unexpected thermal stabilization effect of OxodA on telomeric G-quadruplex DNA prompted us to further investigate the conformation of G-quadruplex DNA (**1**–**9**) in $Na^+$ and $K^+$ solution using CD (Fig. 3). In the presence of 150 mM $Na^+$, the CD spectra of all the G-quadruplex DNA structures (**1**–**9**) showed a strong positive band at 295 nm and a strong negative band between 263 and 267 nm, a characteristic of an antiparallel G-quadruplex conformation [15], although the amplitudes of these peaks vary with respect to different sequences. The intensity of the molar ellipticity of the CD spectra suggests that the sequence may not form the same amount of structured quadruplex [16]. Our observation suggested that the presence of OxodA in the loops does not alter the topology of telomeric G-quadruplex DNA in $Na^+$. The conformational structures of telomeric G-quadruplex DNAs in $K^+$ are much more complex as compared to those in $Na^+$. In the presence of 150 mM KCl, all G-quadruplex DNA (**1**–**9**) showed a strong positive peak around 288–293 nm with a different amplitude for each DNA. All DNAs except for DNA **9** also showed a small negative peak at 235 nm. In contrast, the CD spectrum of DNA **9** between 235–245 nm gave a plateau. The shapes of CD spectra in the region of 240–260 nm represent the most distinct differences. For DNA **1**, **2**, **4**, **5**, **7** and **8**, a positive wave between 248 and 258 nm appeared as a shoulder peak. In addition, DNA **2** showed another shoulder peak around 272 nm. Instead of a flat shoulder peak as DNA **1**, DNA **3** displayed a positive peak at 250 nm. It is noteworthy that DNA **3** also gave the highest positive peak at 293 nm. DNA **6** showed a positive peak at 247 nm and a small negative peak at 262 nm. DNA **9** displayed a negative peak at 258 nm. The differences in the CD spectra described above suggest various conformations of G-quadruplex DNA **1**–**9** in $K^+$.

The conformations of DNA **1**–**9** were further determined using native PAGE. Regardless of the cations in solution, all G-quadruplex DNAs under our conditions formed a predominant conformational structure because only one major band for each DNA was observed (Fig. 3). In our experiments, the gel mobility of G-quadruplex DNA **1**–**9** in $Na^+$ was exactly the same, suggesting the same conformational structure that is consistent with the CD results. On the other hand, clear differences in gel mobility of G-quadruplex **1**–**9** in $K^+$ were observed (Fig. 3). DNA **4** and **6** had similar mobility to DNA **1**. DNA **9** also moved slightly faster than DNA **1** while DNA **3**, **5**, **7**, and **8** moved slower than DNA **1**. DNA **5** had the least mobility amongst all nine G-quadruplex DNAs. DNA **2** containing OxodA at the 5′ end moved much faster than other DNAs that contain OxodA in the loop(s). This variation in mobility suggests that the conformations of G-quadruplexes are different in $K^+$ solution.

### 3.3. Thermodynamic energies of G-quadruplex DNA containing OxodA in the loops

The G-quadruplex sequences (Fig. 1) for calculations contain an extra deoxythymidine (dT) at the 5′ position as compared to DNA **1**. The high resolution G-quadruplex structure (pdb id: 2jsm) of this sequence has been determined by NMR [17], which is used as a reference in our calculations. The G-quadruplexes optimized around adenine 20, 14, and 8 are designated as **GQ20**, **GQ14**, and **GQ8**, respectively. The number represents the location of dA in the sequence (Fig. 1). Each loop consists of a 5′ TTA sequence. When dA at position 8, 14, and 20 is replaced by OxodA, the corresponding DNAs are named as **GQ8OA**, **GQ14OA**, and **GQ20OA**, respectively. The potassium ion bound structures are labeled with **$K^+$** at the end of each name such as **GQ20$K^+$**, **GQ20OA$K^+$**, **GQ14$K^+$**, and **GQ14OA$K^+$**. Thermodynamic energies for all three loops with or without $K^+$ binding are listed in Table 2. $\Delta E_1$ represents the energy difference in G-quadruplex structures when OxodA replaces dA in a single loop. $\Delta E_2$ represents the energy difference in unmodified G-quadruplex structures with and without $K^+$ binding. $\Delta E_3$ represents the energy difference in G-quadruplex structures containing OxodA with and without $K^+$ binding. $\Delta E_4$ represents the overall energy difference between unmodified G-quadruplex DNA and modified G-quadruplex DNA in the case of $K^+$ binding.

**Table 2**
Reaction energies (in kcal/mol) for **GQ20**, **GQ14**, **GQ8** at the ONIOM(B3LYP/6-311++G(2d,p):UFF)//ONIOM(B3LPY/6-31G(d):UFF) level.

| GQ | $\Delta E_1$ (kcal/mol) | $\Delta E_2$ (kcal/mol) | $\Delta E_3$ (kcal/mol) | $\Delta E_4$ (kcal/mol) |
|---|---|---|---|---|
| GQ20 | 1.3 | −230.9 | −238.8 | −6.6 |
| GQ14 | 28.8 | −182.4 | −210.1 | 1.1 |
| GQ8 | 31.4 | – | – | – |

GQ + OA → GQOA + A, $\Delta E_1$; GQ + $K^+$ → GQ$K^+$, $\Delta E_2$; GQOA + $K^+$ → GQOA$K^+$ + A, $\Delta E_3$; GQ$K^+$ + OA → GQOA$K^+$ + A, $\Delta E_4$.

## 4. Discussion

### 4.1. OxodA in the loops stabilizes G-quadurplex DNA

Effect of native DNA lesions on G-quadruplex DNA received far less attention as compared to that on duplex DNA. Available reports so far are only limited to OxodG [8] and an abasic site mimic [9,10]. We believe that it is necessary to extend such studies because DNA lesions could have significant impact on biophysical and biochemical properties of G-quadruplex DNA. In this study, OxodA was chosen to replace dA in a human telomeric G-quadruplex DNA sequence $d[AG_3(T_2AG_3)_3]$ as it is a major oxidation product of dA [18]. In our studies, OxodAs do not participate in the G-quartet formation because dAs are only present in the TTA loops of this G-quadruplex DNA.

Our results showed that the melting temperatures of G-quadruplex DNAs are independent of DNA concentrations, clearly indicating the formation of intramolecular G-quadruplex structures [12]. In addition, the melting and annealing curves showed no hysteresis, suggesting that the association/dissociation processes are at thermodynamic equilibrium [19]. Based on the melting temperatures, the following trends can be derived: (1) The presence of OxodA at 5′ (DNA **2**) stabilizes G-quadruplex DNA. (2) The presence of OxodA in loop 1 (DNA **3**), especially in $Na^+$, slightly destabilizes G-quadruplex DNA. (3) The presence of OxodA in loop 2 and 3 (DNA **4**, **5**, and **8**) stabilizes G-quadruplex DNA. (4) The presence of OxodA in loop 2 and 3 dictates the stability of G-quadruplex regardless of OxodA in loop 1 (DNA **6**, **7**, and **9**). Collectively, it can be concluded that OxodA in loop 2 and 3 enhances the stability of G-quadruplex DNA especially in the presence of $K^+$ but OxodA in loop 1 may slightly decrease the stability of G-quadruplex DNA. The stabilization effect observed by us is quite significant because only very small structural variation is present between dA and OxodA. Sugimoto and co-workers reported a similar observation in which single base change in a loop could have a drastic effect on G-quadruplex stability and structure. However, in their study a TTA loop was changed into a TTG loop and the experiments were conducted under molecular crowding conditions [20]. The stabilization effect is more drastic in $K^+$ solution than in $Na^+$ solution at the concentrations ranging from 10 to 110 mM. The observations at 110 mM $K^+$ are particularly important, as this is the physiologically relevant concentration in human cells.

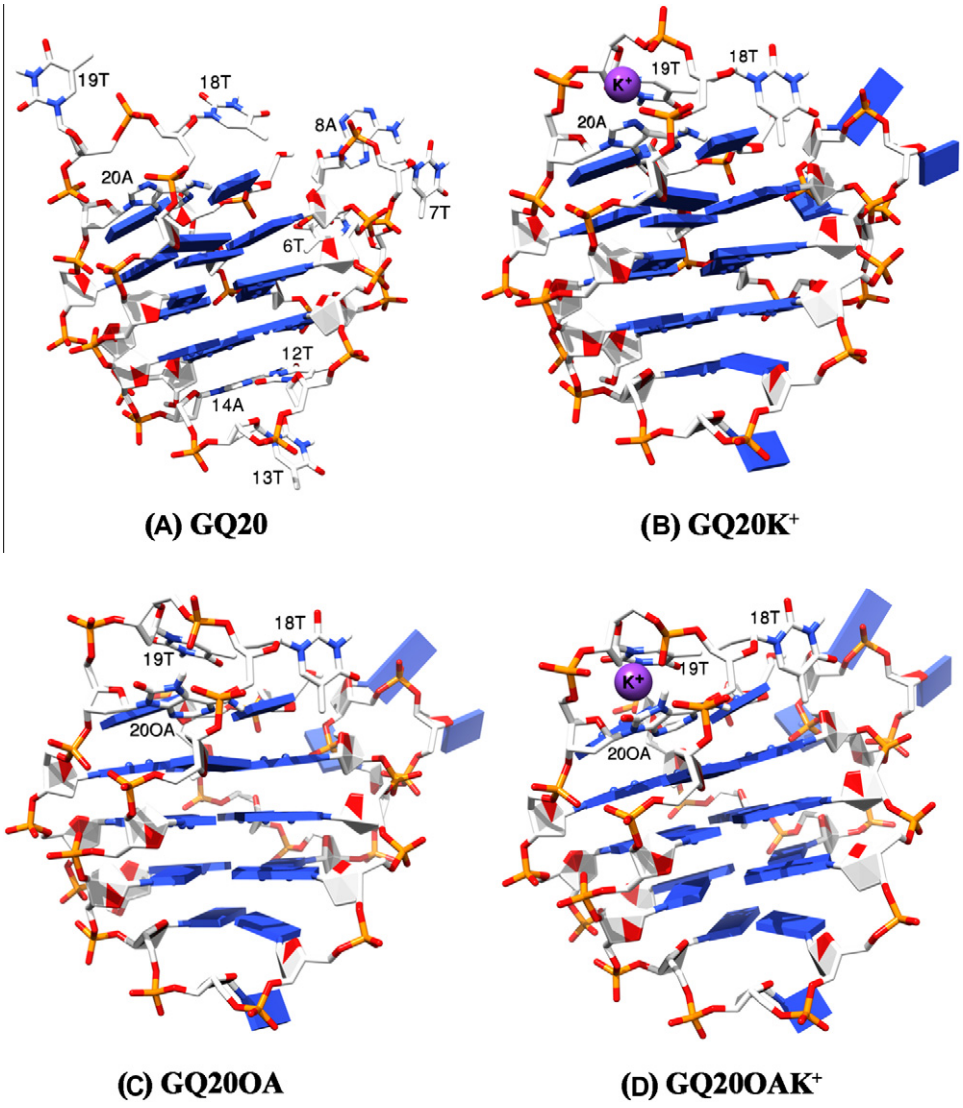


**Fig. 4.** Optimized structures of G-quadruplexes in ONIOM(B3LYP/6-31G(d):UFF) level. (A) **GQ20**, G-quadruplex with residues 18T, 19T, and 20A are optimized at the QM level, (B) **GQ20K$^+$**, $K^+$ complexes with **GQ20**; (C) **GQ20OA**, Adenine 20 mutated to OA; and (D) **GQ20OAK$^+$**, $K^+$ complexes with **GQ20OA**. The positions of dAs are labeled on top of sequences. **OA** = OxodA.

As shown in Table 1, thermodynamic values of DNA **2**, **8** and **9** in 110 mM $Na^+$ suggest unfavorable enthalpy changes and enthalpy–entropy compensation effects are present in all three cases. Only these three DNAs are exclusively considered here because they display the stabilization effect in the presence of $Na^+$. In 110 mM $K^+$, thermodynamic values of all DNAs gave favorable enthalpy changes but unfavorable entropy changes. The increased enthalpy change values may originate from conformational changes that result in better stacking capacity between the G-quartets and/or the loops. The decreased entropy change values may indicate more organized conformations formed in the presence of $K^+$. The larger enthalpic contribution that is accompanied by less flexibility, maybe by forming more or ordered loop structures, has been previously observed [21,22]. Plausible explanation will be proposed using computer modeling in the section below.

### 4.2. Conformations are different in $Na^+$ and $K^+$

The stabilization effect of OxodA on G-quadruplex DNA mentioned above is striking because modified bases present in the loops do not involve in the G-quartet formation that is believed to be a predominant factor for stabilizing G-quadruplex DNA. Furthermore, OxodA only has a very small structural variation as compared to dA. How can such a seemly trivial variation in the loops enhance the stability of G-quadruplex DNA? To address it, we sought to make a comparison of the conformations of G-quadruplex DNA **1**–**9** using circular dichroism, which is a convenient means to survey the conformation of G-quadruplex with similar structures. Incorporation of OxodA into any loop position of the 22-mer d[$AG_3(T_2AG_3)_3$] did not alter its CD spectrum in NaCl with two characteristic 295 and 265 nm peaks, indicating that all DNA **1**–**9** in $Na^+$ fold into an antiparallel G-quadruplex conformation [23]. In addition, such a conformation should be predominant in $Na^+$ because native PAGE results showed only one major band with similar mobility for each DNA (Fig. 3).

The CD spectra of DNA **1**–**9** in $K^+$ are drastically different from those in $Na^+$. None of the G-quadruplex DNA shows the parallel conformation that is commonly observed for the human telomeric sequence of d[$AG_3(T_2AG_3)_3$] because they all lack of a positive signal at 265 nm and a negative signal at 240 nm [15]. It is well-known that intramolecular G-quadruplex DNA can have complex conformations in $K^+$. Chaires and co-workers reported that the

structure of telomeric G-quadruplex in $K^+$ could be different from the crystal structure based on sedimentation and fluorescence studies [24]. Recent studies revealed several novel conformational structures of telomeric G-quadruplex DNA in $K^+$, implying that telomeric G-quadruplex DNA may have a complex structure–function relationship [7]. Sugiyama and coworkers proposed new models of $d[AG_3(T_2AG_3)_3]$ in $K^+$ solution [25]. Their CD spectra are similar to ours, suggesting that our DNA **1**–**9** in $K^+$ exist as a mixture of mixed-parallel/antiparallel and chair-type G-quadruplex. It is clear that OxodA in the loops promotes the formation of different conformational structures of telomeric G-quadruplex DNA in $K^+$. But the effect of OxodA on G-quadruplex conformations in $Na^+$ is not significant. Further evidence for this conclusion comes from the PAGE experiments. Since the DNA sequences used in our study were the same length and had very close molecular weights (only 1–3 oxygen atom difference), any mobility difference in PAGE should result from the conformational differences. As shown in Fig. 3, the mobility of DNA **1**–**9** in $K^+$ is clearly not uniform. It seems that OxodA at the 5' position of the DNA (DNA **2**) makes it the highest mobility and OxodA present in loop 3 slows down the mobility of the corresponding DNA (DNA **5**, **7**, and **8**). Nevertheless, it is necessary to point it out that no defined correlation between gel mobility and CD spectra can be established at this point.

### 4.3. Possible stabilization factor elucidated by computer modeling

In light of the findings from our biophysical measurements, the unusual stability of G-quadruplex DNA containing OxodA was further analyzed using computational calculations. Representative optimized structures for **GQ20** and **GQ20OA** (OxodA in loop 3) and their $K^+$ complexes are presented in Fig. 4. The three loop regions are shown as stick representation and labeled in Fig. 4(A). The loop consisting of 18T, 19T and 20A forms a nice pocket with three oxygen atoms from phosphates making electron density very high. The hydrogen atom (H1′) on 20A is pointing toward the pocket. The mutation of 20A to OxodA will increase electron density in the pocket, and introduce a new hydrogen atom on N7 that can form hydrogen bonding with an oxygen atom in phosphate group on 18T. Increasing electron density in the loop region will be a negative effect on stability but the extra hydrogen bonding could compensate this repulsion to some extent. Based on these analyses, the stability on mutation in this loop is decreased by 1.3 kcal/mol, which is obviously contradictory to our observed stabilization effect. When the $K^+$ binding is considered; however, this mutation gives a completely different picture. The binding energy of $K^+$ with **GQ20OA** is 7.9 kcal/mol larger than that with **GQ20**, indicating that the mutation of 20A to OxodA generates a much better binding pocket to $K^+$. Overall, **GQ20OAK$^+$** is 6.6 kcal/mol more stable than **GQ20K$^+$**. This computational result is consistent with our experimental data that stabilization by OxodA is most significant in the presence of $K^+$. The less stabilization effect in the presence of $Na^+$ in part because the binding of the mutated pocket to $Na^+$ may not be as fit as to $K^+$.

Adenines in other loops are also replaced by OxodAs for similar calculations. Adenine 14A (in loop 2) is located in the loop forming a major groove and does not form a well-defined pocket. Also, there are hydrogen bondings between 12T and 14A base pairs. On substitution of 14A with OxodA, the base pair loses one hydrogen bonding interaction and introduces new repulsions between the two hydrogens on OA and 12T. All these negative effects of the substitution destabilize 28.8 kcal/mol. However, the binding energy of $K^+$ with **GQ14OA** (OxodA in loop 2) is 27.7 kcal/mol stronger than with **GQ14**; therefore, the overall stability of **GQ14K$^+$** over **GQ14OAK$^+$** is 1.1 kcal/mol in the model system. In real $K^+$ solution, such a small stabilization energy could be easily surpassed and the trend of stability may be reversed because more $K^+$ cations can interact with this loop and the O8 of OxodA can enhance coordination with multiple $K^+$, making **GQ14OAK$^+$** more stable than **GQ14K$^+$**. The last mutation we tested in the model system was 8A (**GQ8**), and the destabilization by substitution (**GQ8OA**, OxodA in loop 1) was 31.4 kcal/mol that is even larger than **GQ14**. The bases on the loop were not ordered, and the binding complex with $K^+$ was not located at the level of theory applied. This result is also consistent with our thermal denaturation data that the presence of OxodA in loop 1 slightly destabilizes G-quadruplex DNAs.

Based on the computational results, plausible factors for G-quadruplex stabilization effect by OxodA are drawn as follows: the stabilization of G-quadruplex DNA when OxodA is present in loop 2 and 3 may result from the tight binding of cations in the pocket. Binding of $K^+$ to loop 1 containing OxodA seems not plausible and the enhanced electron density results in a destabilization effect without the compensation from $K^+$ binding.

## 5. Conclusions

In summary, the stabilization of G-quadruplex DNA by OxodA present in the loops in the presence of monovalent cations ($Na^+$ and $K^+$) was characterized using biophysical methods and plausible stabilization factors were elucidated using computer modeling. It is necessary to point it out that other stabilization factors such as molecular flexibility around OxodA and base-pairing interactions of OxodA with neighboring nucleobases are plausible. Our studies are in line with previous reports that the nature of the loops plays a key role in determining the topology and stability of G-quadruplexes. Reported here is the first example of G-quadruplex stabilization by a native DNA lesion, which warrants further investigation.

## Acknowledgment

We are grateful for support of this research from the University of the Pacific.

## Appendix A. Supplementary data

Experimental details for UV melting profiles and thermodynamic parameter calculations are described in the Supporting Information. Supplementary data associated with this article can be found, in the online version, at http://dx.doi.org/10.1016/j.bbrc.2012.04.059.

## References

[1] S. Burge, G.N. Parkinson, P. Hazel, A.K. Todd, S. Neidle, Survey and summary quadruplex DNA: sequence, topology and structure, Nucleic Acids Res. 34 (2006) 5402–5415.
[2] J.L. Huppert, S. Balasubramanian, Prevalence of quadruplexes in the human genome, Nucleic Acids Res. 33 (2005) 2908–2916.
[3] A.K. Todd, M. Johnston, S. Neidle, Highly prevalent putative quadruplex sequence motifs in human DNA, Nucleic Acids Res. 33 (2005) 2901–2907.
[4] K.C. Healy, Telomere dynamics and telomerase activation in tumor progression–prospects for prognosis and therapy, Oncol. Res. 7 (1995) 121–130.
[5] J.L. Mergny, P. Mailliet, F. Lavelle, J.F. Riou, A. Laoui, C. Helene, The development of telomerase inhibitors: the G-quartet approach, Anticancer Drug Des. 14 (1999) 327–339.
[6] S. Neidle, G. Parkinson, Telomere maintenance as a target for anticancer drug discovery, Nat. Rev. Drug Discov. 1 (2002) 383–393.
[7] D. Yang, K. Okamoto, Structural insights into G-quadruplexes: towards new anticancer drugs, Future Med. Chem. 2 (2010) 619–646.
[8] V.A. Szalai, M.J. Singer, H.H. Thorp, Site-specific probing of oxidative reactivity and telomerase function using 7,8-dihydro-8-oxoguanine in telomeric DNA, J. Am. Chem. Soc. 124 (2001) 1625–1631.
[9] M. Cevec, J. Plavec, Role of loop residues and cations on the formation and stability of dimeric DNA G-quadruplexes, Biochemistry 44 (2005) 15238–15246.

[10] P. Skolakova, K. Bednarova, M. Vorlickova, J. Sagi, Quadruplexes of human telomere dG3(TTAG3)3 sequences containing guanine abasic sites, Biochem. Biophys. Res. Commun. 399 (2010) 203–208.
[11] L.W. Chung, H. Hirao, X. Li, K. Morokuma, The ONIOM method: its foundation and applications to metalloenzymes and photobiology, Wiley Interdiscip. Rev. Comput. Mol. Sci. 2 (2012) 327–350.
[12] J.L. Mergny, L. Lacroix, UV melting of G-quadruplexes, Curr. Protoc. Nucleic Acid Chem. 37 (2009). 17.1.11–17.1.15.
[13] Supporting Information.
[14] A. Risitano, K.R. Fox, Stability of intramolecular DNA quadruplexes: comparison with DNA duplexes, Biochemistry 42 (2003) 6507–6513.
[15] P. Balagurumoorthy, S.K. Brahmachari, Structure and stability of human telomeric sequence, J. Biol. Chem. 269 (1994) 21858–21869.
[16] V. Esposito, L. Martino, G. Citarella, A. Virgilio, L. Mayol, C. Giancola, A. Galeone, Effects of abasic sites on structural, thermodynamic and kinetic properties of quadruplex structures, Nucleic Acids Res. 38 (2009) 2069–2080.
[17] A.T. Phan, V. Kuryavyi, K.N. Luu, D.J. Patel, Structure of two intramolecular G-quadruplexes formed by natural human telomere sequences in $K^+$ solution, Nucleic Acids Res. 35 (2007) 6517–6525.
[18] M.D. Evans, M. Dizdaroglu, M.S. Cooke, Oxidative DNA damage and disease: induction, repair and significance, Mutat. Res. 567 (2004) 1–61.
[19] E.E. Merkina, K.R. Fox, Kinetic stability of intermolecular DNA quadruplexes, Biophys. J. 89 (2005) 365–373.
[20] D. Miyoshi, H. Karimata, N. Sugimoto, Drastic effect of a single base difference between human and tetrahymena telomere sequences on their structures under molecular crowding conditions, Angew. Chem. Int. Ed. 44 (2005) 3740–3744.
[21] P.A. Rachwal, T. Brown, K.R. Fox, Sequence effects of single base loops in intramolecular quadruplex DNA, FEBS Lett. 581 (2007) 1657–1660.
[22] I. Smirnov, R.H. Shafter, Effect of loop sequence and size on DNA aptamer stability, Biochemistry 39 (2000) 1462–1468.
[23] Y. Wang, D.J. Patel, Solution structure of the human telomeric repeat $d[AG_3(T_2AG_3)_3]$ G-tetraplex, Structure 1 (1993) 263–282.
[24] J. Li, J.J. Correia, L. Wang, J.O. Trent, J.B. Chaires, Not so crystal clear: the structure of the human telomere G-quadruplex in solution differs from that present in a crystal, Nucleic Acids Res. 33 (2005) 4649–4659.
[25] Y. Xu, Y. Noguchi, H. Sugiyama, The new models of the human telomere d[AGGG(TTAGGG)3] in $K^+$ solution, Bioorg. Med. Chem. 14 (2006) 5584–5591.